Ultrasonics 132 (2023) 107010

Contents lists available at ScienceDirect

Ultrasonics

journal homepage: www.elsevier.com/locate/ultras

Short communication

# Optimal transmit apodization for the maximization of lag-one coherence with applications to aberration delay estimation

Rehman Ali [a,*], Nebojsa Duric [a], Jeremy J. Dahl [b]

[a] University of Rochester Medical Center, Rochester, NY, 14642 USA

[b] Department of Radiology, Stanford University School of Medicine, Palo Alto, CA, 94304 USA

ARTICLE INFO

*Keywords:*
Phase aberration correction
Nearest-neighbor cross correlation
Lag-one coherence
van Cittert Zernike theorem

ABSTRACT

Phase aberration is one of the major sources of image degradation in medical ultrasound imaging. One of the earliest and simplest techniques to correct for phase aberration involves nearest-neighbor cross correlation to estimate delays between neighboring receive channels and the compensation of aberration delays in a delay-and-sum beamformer. The main challenge is that neighboring receive channels may not have sufficient signal correlation to accurately estimate the aberration delays. Although algorithms such as the translating transmit aperture or the common midpoint gather are designed to perfectly maximize signal correlations between received signals, these algorithms require the use of different transmit apertures for each received signal. Instead, this work proposes the use of a single globally-applicable transmit apodization function that optimizes the lag-one coherence based on the van Cittert–Zernike theorem. For the application to phase aberration correction, it is shown across 20 different zero-mean Gaussian-random aberrators that the proposed optimal apodization function reduces the estimation error in the aberration delay profile from 22.85% to 15.72%.

## 1. Introduction

Phase aberration remains one of the key sources of image degradation in medical ultrasound imaging alongside reverberation and off-axis clutter [1]. Aberration is the result of spatial variations in the speed of sound that cause a delaying and advancing of the wavefront to produce a misalignment of signals across the aperture. The simplest model used to correct for phase aberration is the near-field phase screen [2–4]. Under this model, all phase aberration is assumed to take place on a thin film at the transducer surface, and a single set of element-wise delays will compensate for this thin film at all points in the ultrasound image (i.e., an infinite isoplanatic patch). However, in most *in vivo* imaging cases, any set of compensating delays will have a finite isoplanatic patch, which is roughly defined as the imaging region over which that set of compensating delays will correct for aberrations in the ultrasound image. In practice, the isoplanatic patch depends on the sound speed distribution in tissue. This results in a patch-wise correction approach [5,6].

One of earliest and simplest methods to estimate aberration delays from received ultrasound signals was nearest-neighbor cross correlation [2,4]. However, the main difficulty associated with nearest-neighbor cross correlation is the lack of signal correlation to optimally estimate aberration delays. One of the approaches that overcomes this limitation is the common midpoint gather [3,7,8], in which all single-element transmit-and-receive channel pairs that share a common midpoint have a correlation very close to 1, regardless of the scattering distribution. However, because this approach requires both a changing transmit and receive aperture, it becomes necessary to model the aberration between any two measurements as being the sum of aberrations accumulated on both transmission and reception. This results in a large number of cross-correlation measurements in an over-determined system of equations to solve for a single set aberration delays [7]. This two-way modeling of phase aberration also increases the complexity of ray tomography for sound speed estimation in pulse-echo ultrasound [9].

For these reasons, most of the aberration correction literature relies on a one-way modeling of aberration delay [4]. Nearest neighbor cross correlation fell out of favor because of the low signal-to-noise ratio (SNR) on individual receive channels and the accumulation of error when integrating over differential measurements. For this reason, the beamsum method [10] became a popular choice: by comparing individual receive channels to the beamsum, the SNR of the measurement improved and it was no longer necessary to integrate over differential measurements.

However, the context has since changed. Improvements in acquisition hardware and transducer design have improved the SNR over individual receive channels. Various transmit encoding schemes and

* Corresponding author.
*E-mail address:* Rehman_Ali@URMC.Rochester.edu (R. Ali).

https://doi.org/10.1016/j.ultras.2023.107010
Received 2 September 2022; Received in revised form 22 March 2023; Accepted 8 April 2023
Available online 23 April 2023

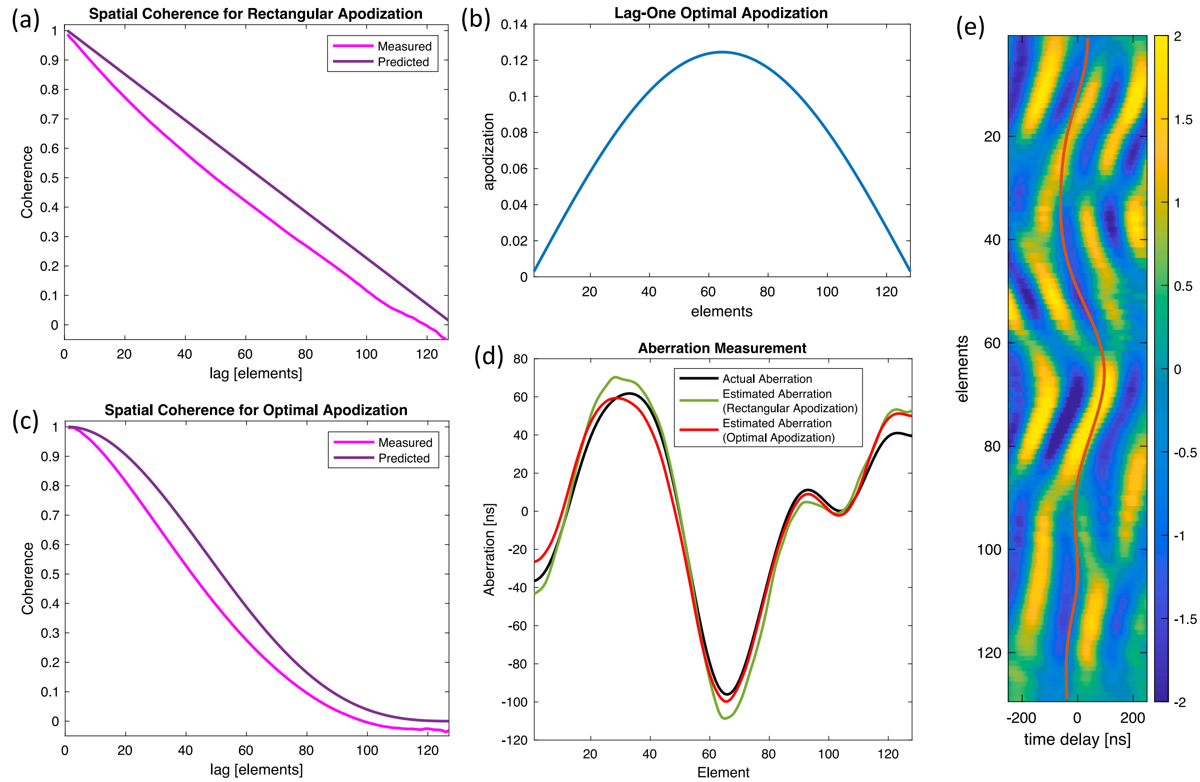


**Fig. 1.** Comparison of Lag-One Optimal and Rectangular Apodizations. (a) Measured vs. theoretical signal coherence as functions of lag (or element offset) for a rectangular apodization. (b) Lag-one optimal apodization based on Algorithm 1. (c) Measured vs. theoretical signal coherence functions for the lag-one optimal apodization. (d) Example estimate of aberration delays using each apodization. (e) These signals vs. time were correlated between nearest-neighbor receive-element pairs to estimate the aberration delay. The estimated aberration delay profile was plotted over the signal traces.

synthetic aperture reconstruction techniques [11–14] have also been shown to further improve SNR. The advent of the software beamformer enables several other filtering techniques [15–17] to remove the impact of incoherent noise and reverberation clutter from received channel data.

In this context where SNR is no longer the limiting factor, we reconsider approaches that rely on correlations between individual receive channels. We reconsider nearest neighbor cross-correlation because the van-Cittert Zernike (VCZ) theorem [18] predicts the highest correlation between neighboring receive elements ($\rho = \frac{N-1}{N}$ for an N-element transducer with rectangular transmit apodization). The correlation between neighboring receive elements is also the most robust to cycle skipping, especially in comparison to the beamsum method where larger delays would be measured between each receive channel and the beamsum. According to the VCZ theorem, the correlation between each receive channel and the beamsum would range from 0.5 to 0.75 from the edges to the center of the receive aperture; this is much lower than the correlation between neighboring receive channels. Additionally, sound speed estimation [9] requires modeling the differential delay between individual receive channels in terms of the sound speed profile in tissue.

Regardless, the issue remains that the accumulation of differential measurements from nearest neighbor cross correlation would continue to accrue errors. The correlation between neighboring receive elements compounded over the receive aperture for a rectangular transmit apodization would be $\rho^{N-1} = \left(\frac{N-1}{N}\right)^{N-1} \approx \frac{1}{e} \approx 0.37$, which is considerably lower than the 0.5–0.75 seen with the beamsum method. This short communication aims to introduce a method to find the optimal transmit apodization that maximizes the correlation $\rho$ between neighboring receive channels, bringing $\rho^{N-1}$ much closer to 1.

## 2. Theory

The framework used to derive the optimal transmit apodization for nearest-neighbor cross correlation is based on the maximization of lag-one coherence (LOC), which already has several applications related to image quality assessment and the suppression of incoherent reverberation [19]. For a single transmit aperture, the VCZ theorem [18] in pulse-echo ultrasound imaging predicts that the correlation of received signals is given by the autocorrelation of the transmit apodization function.

We define the lag-one optimal apodization as the transmit apodization that maximizes the correlation between echoes measured from neighboring receive elements on the array. According to the VCZ theorem [18], the correlation between neighboring receive channels is the lag-one autocorrelation of the transmit apodization. Given a vector of apodization weights $\vec{w} = [w_1, \ldots, w_N]^T$ for an $N$-element transducer, its autocorrelation $\rho_n$ at lag $n$ is

$$\rho_n = \vec{w}^T A_n \vec{w},$$

where $A_n$ is a matrix where the $n$th diagonal is all ones and remaining entries of the matrix are zero (e.g., $A_0$ is the identity matrix, $A_1$ only has ones on the first superdiagonal, and $A_{-1}$ only has ones on the first subdiagonal):

$$A_0 = \begin{bmatrix} 1 & 0 & & 0 \\ 0 & 1 & \ddots & \\ & \ddots & \ddots & 0 \\ 0 & & 0 & 1 \end{bmatrix}, \quad A_1 = \begin{bmatrix} 0 & 1 & & 0 \\ 0 & 0 & \ddots & \\ & \ddots & \ddots & 1 \\ 0 & & 0 & 0 \end{bmatrix},$$

$$A_{-1} = \begin{bmatrix} 0 & 0 & & 0 \\ 1 & 0 & \ddots & \\ & \ddots & \ddots & 0 \\ 0 & & 1 & 0 \end{bmatrix}.$$

Note that $\rho_n = \rho_{-n}$. The optimal apodization should minimize $\rho_0 - \rho_1$ subject to the constraint that $\|\vec{w}\| = 1$. However to ensure the symmetric positive definiteness of this optimization problem, $2\rho_0 - \rho_1 - \rho_{-1}$ is minimized instead:

$$\underset{x}{\text{minimize}} \quad 2\rho_0 - \rho_1 - \rho_{-1} = \vec{w}^T(2A_0 - A_1 - A_{-1})\vec{w},$$

$$\text{subject to} \quad \vec{w}^T\vec{w} = \sum_{n=1}^{N} w_n^2 = 1.$$

where $2A_0 - A_1 - A_{-1}$ is simply a tri-diagonal Toeplitz matrix with diagonals $[-1, 2, -1]$:

$$2A_0 - A_1 - A_{-1} = \begin{bmatrix} 2 & -1 & & 0 \\ -1 & 2 & \ddots & \\ & \ddots & \ddots & 1 \\ 0 & & -1 & 2 \end{bmatrix}.$$

The constraint on this optimization problem makes it non-convex, so sequential convex programming is used to relax the constraint to $\vec{w}_{prev}^T\vec{w} = 1$, where $\vec{w}_{prev}$ is the solution for $\vec{w}$ from the previous iteration of the same problem after normalizing $\vec{w}$ to a length of 1:

$$\underset{x}{\text{minimize}} \quad 2\rho_0 - \rho_1 - \rho_{-1} = \vec{w}^T(2A_0 - A_1 - A_{-1})\vec{w},$$

$$\text{subject to} \quad \vec{w}_{prev}^T\vec{w} = 1.$$

The complete algorithm is shown in Algorithm 1. In the presence of an aberrator with known phase aberrations $\phi_n$ over each element, the optimal apodization would be complex-valued: $w_n e^{-j\phi_n}$ where the magnitude $w_n$ is the same as the apodization obtained from Algorithm 1, and the phase $-\phi_n$ would compensate for the aberration over the transmit aperture. However, in practice the phase aberrations $\phi_n$ over each element are not known a-priori. We assume that the aberration is zero mean such that Algorithm 1 would maximize the lag-one coherence over a large ensemble of random aberrators and speckle realizations. Although this leads to a submaximal lag-one coherence over individual aberrator realizations, the lag-one coherence remains maximal over the ensemble.

**Algorithm 1** Iterative Algorithm for Obtaining the Lag-One Optimal Transmit Apodization

Random Initialization for $\vec{w}_0$
**while** $|\|\vec{w}_k\| - 1| > \epsilon$ and $\left|\frac{\lambda_k - \lambda_{k-1}}{\lambda_k}\right| > \epsilon$ **do**
    $\vec{w}_k \leftarrow \vec{w}_k / \|\vec{w}_k\|$
    $\begin{bmatrix} \vec{w}_{k+1} \\ \lambda_{k+1} \end{bmatrix} \leftarrow \begin{bmatrix} 2A_0 - A_1 - A_{-1} & \vec{w}_k \\ \vec{w}_k^T & 0 \end{bmatrix}^{-1} \begin{bmatrix} \vec{0} \\ 1 \end{bmatrix}$
    $k \leftarrow k + 1$
**end while**
**return** $\vec{w}_k$

Algorithm 1 can also be generalized such that $2A_0 - A_1 - A_{-1}$ is replaced by $2N_{lags}A_0 + \sum_{n=1}^{N_{lags}} A_n + A_{-n}$ to create an apodization that is optimal up to lag $N_{lags} \ll N$. Note that as $N_{lags}$ approaches $N$, the optimal apodization will reduce to the rectangular apodization function, so the main benefit of this scheme will only be for short lags (i.e., $N_{lags} \ll N$). This short communication mainly considers $N_{lags} = 1$ to maximize the lag-one coherence and optimize nearest-neighbor cross-correlation for aberration delay measurements. The following MATLAB code provides the implementation for the transmit apodization that is optimal up to lag $N_{lags}$: https://github.com/rehmanali1994/IMPACT/blob/main/MATLAB/functions/optApod.m.

## 3. Methods

Field II [20,21] was used to simulate diffuse scattering in a 3D volume ranging from the plane of the transducer to 40 mm depth from

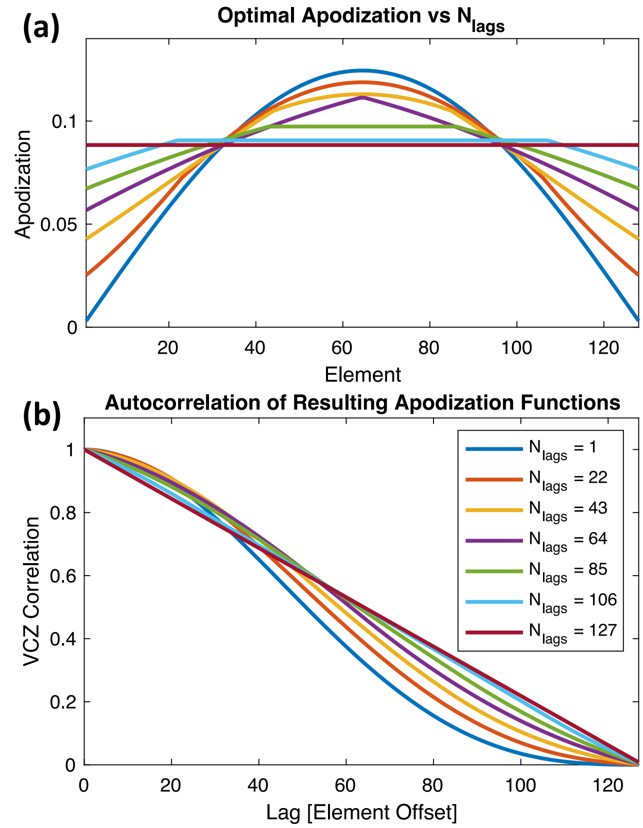


**Fig. 2.** Apodizations Optimal Up to $N_{lag}$ and Resulting Spatial Coherence Functions. (a) As $N_{lag}$ increases from 1 to $N-1$, the optimal apodization approaches the rectangular apodization. (b) The resulting spatial coherence function approaches the triangle function.

a multistatic synthetic aperture acquisition on a 128-element linear-array transducer with 0.2 mm pitch. However, spatial coherence and aberration delays were evaluated at 20 mm depth. The transmit pulse had a center frequency of 5 MHz and a 70% fractional bandwidth. The purpose of this initial simulation was to demonstrate agreement between the predicted and actual spatial coherence (functions of lag or element offset) when using either a rectangular apodization or the lag-one optimal apodization.

An additional 20 Field II simulations were used to simulate diffuse scattering the presence of a near-field phase screen. The purpose of these simulations were to quickly demonstrate the impact of the lag-one optimal apodization on the estimation of aberration delays. Aberration delays were estimated using nearest-neighbor cross-correlation [2,4]. Each Field II simulation was used to simulate a different 50 ns root-mean-square (RMS) Gaussian-random aberrator with a correlation length of 4 mm in a 1540 m/s medium. The accuracy of the estimated aberration delay profile was assessed using RMS error. A normalized RMS error was obtained by using the RMS strength of the true aberration delay profile as the normalization factor.

## 4. Results and discussion

Fig. 1 compares the lag-one optimal apodization scheme to the application of a conventional rectangular apodization for nearest-neighbor cross-correlation measurements over a 128-element transducer ($N = 128$). Fig. 1(a) shows the measured spatial coherence as a function of lag (or element offset) compared to the result predicted by VCZ theorem for a rectangular transmit apodization. Fig. 1(b) shows the lag-one optimal apodization, and Fig. 1(c) compares the measured spatial coherence to the VCZ theorem prediction for the lag-one optimal

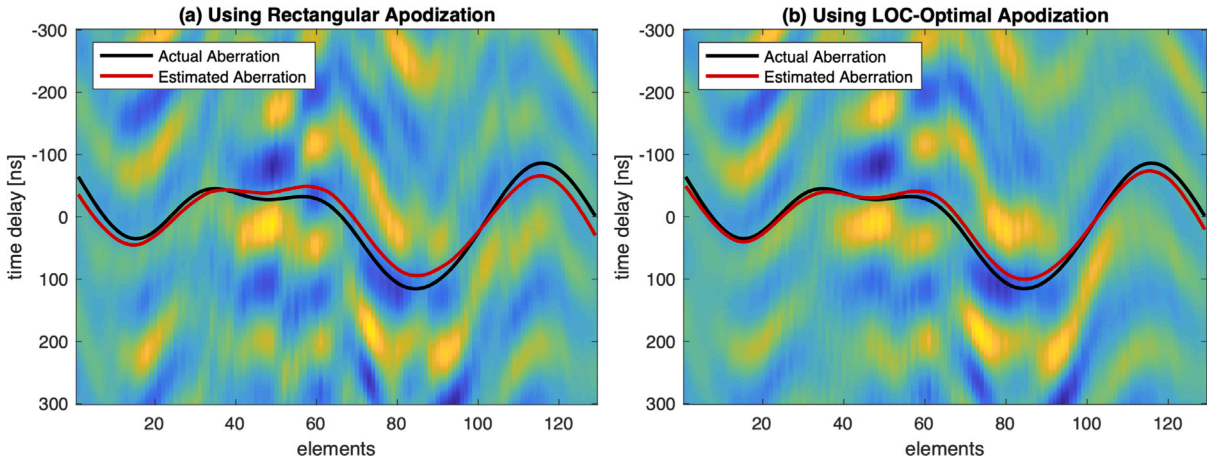


**Fig. 3.** Impact of (a) the rectangular apodization and (b) the LOC-optimal apodization on the correlation of received signals for a speckle generating phantom aberrated by a near-field phase screen. The LOC-optimal apodization improves the smoothness of received signals across the aperture. In this example, the root-mean-square (RMS) error in the aberration delay measurement is 17.1844 ns in (a) and 10.7908 in (b). The LOC-optimal apodization improves the accuracy of the aberration delay measurement.

apodization. In both the rectangular and lag-one optimal apodization cases, any discrepancy between the measured and predicted spatial coherence function is the result of applying the VCZ theorem to echoes that originated in the near field since the VCZ theorem was developed using far-field approximations. Regardless of these differences, the lag-one optimal apodization raises the spatial coherence over the short lags at the expense of coherence at very large lags. Fig. 2 shows the optimal apodization and the resulting theoretical spatial coherence function when $N_{lags} > 1$.

For the application to aberration delay estimation, the lag-one optimal apodization reduces the error in the aberration delay measurement (Fig. 1(d)). Averaged across the 20 different zero-mean Gaussian random aberrators, the rectangular apodization resulted in 11.427 ns RMS error (22.85% normalized RMS error) in the aberration delay measurement while the lag-one optimal apodization only has 7.862 ns RMS error (15.72% RMS error) in the aberration delay measurement. The correlation structure of the received signals shown in Fig. 1(e) were impacted by the choice of transmit apodization. Fig. 3 shows that the optimal apodization results in a smoothening of received signals across the aperture. In the presence of aberration, the lag-one coherence is $0.9789 \pm 0.0053$ with rectangular apodization and $0.9855 \pm 0.0069$ with the optimal apodization across the 20 aberrators. A paired t-test at 1% significance level confirms a systematic increase in the lag-one coherence as result of the optimal apodization. These results show the utility of the lag-one optimal apodization for estimation of aberration delays.

This communication demonstrates that the lag-one optimal apodization increases the short-lag spatial coherence of backscattered echoes and increases the accuracy of aberration delay estimation. The lag-one optimal apodization obtained in this work is very similar to the Riesz apodization used in [22] and similar increases in the short-lag spatial coherence are observed. Other apodizations with a similar shape should provide similar improvements in the short-lag spatial coherence and the accuracy of the aberration delay estimates. However, rather than heuristically determining an apodization that increases the LOC, this work derives the lag-one optimal apodization via an optimization problem. For $N = 128$, the optimal apodization achieves a lag-one coherence of $\rho = 0.9997$, and when compounded over the aperture, the result is much closer to 1 ($\rho^{N-1} = 0.963$).

Robust and accurate estimation of aberration delays not only enables phase aberration correction but also enables sound speed estimation via a one-way model of measured aberration delays. The main reason that common mid-angle processing was introduced to sound speed estimation in [9] was to overcome the lack of correlation between signals imaged at different angles of insonification. However, the common mid-angle approach also increased the complexity of ray tomography by requiring a two-way transmit-and-receive model of aberration delays. Additional pre-processing steps such as fan filters also became a requirement for the aberration delay measurement.

## 5. Conclusions

This short communication demonstrates a transmit apodization scheme that maximizes the lag-one coherence based on the van Cittert–Zernike theorem. This optimal apodization is shown to increase the spatial coherence of received echoes over the short lags and improves the accuracy of aberration delay measurements using nearest-neighbor cross correlations. Future work will involve the use of synthetic aperture transmit focusing with the transmit apodization scheme described in this communication to optimally measure aberration delays from received signals and reconstruct the speed of sound in tissue using handheld pulse-echo ultrasound imaging.

## Declaration of competing interest

The authors declare that they have no known competing financial interests or personal relationships that could have appeared to influence the work reported in this paper.

## Data availability

Data will be made available on request.

## Acknowledgments

The research was funded by the National Institute of Biomedical Imaging and Bioengineering (NIBIB) under grants R01EB028652, R01EB027100, and F32EB034589.

## References

[1] G.F. Pinton, G.E. Trahey, J.J. Dahl, Sources of image degradation in fundamental and harmonic ultrasound imaging using nonlinear, full-wave simulations, IEEE Trans. Ultrason. Ferroelectr. Freq. Control 58 (4) (2011).

[2] S. Flax, M. O'Donnell, Phase-aberration correction using signals from point reflectors and diffuse scatterers: Basic principles, IEEE Trans. Ultrason. Ferroelectr. Freq. Control 35 (6) (1988) 758–767.

[3] D. Rachlin, Direct estimation of aberrating delays in pulse-echo imaging systems, J. Acoust. Soc. Am. 88 (1) (1990) 191–198.
[4] G.C. Ng, S.S. Worrell, P.D. Freiburger, G.E. Trahey, A comparative evaluation of several algorithms for phase aberration correction, IEEE Trans. Ultrason. Ferroelectr. Freq. Control 41 (5) (1994) 631–643.
[5] G. Chau, M. Jakovljevic, R. Lavarello, J. Dahl, A Locally Adaptive Phase Aberration Correction (LAPAC) method for synthetic aperture sequences, Ultrason. Imaging (2018) 0161734618796556.
[6] H. Bendjador, S. Décombas-Deschamps, M.D. Burgio, R. Sartoris, B. Van Beers, V. Vilgrain, T. Deffieux, M. Tanter, The SVD beamformer with diverging waves: A proof-of-concept for fast aberration correction, Phys. Med. Biol. 66 (18) (2021) 18LT01.
[7] M.A. Haun, D.L. Jones, W. Oz, Overdetermined least-squares aberration estimates using common-midpoint signals, IEEE Trans. Med. Imaging 23 (10) (2004) 1205–1220.
[8] G.C.-H. Ng, The Application of Translating Transmit Apertures in Adaptive Ultrasonic Imaging, Duke University, 1997.
[9] P. Stähli, M. Kuriakose, M. Frenz, M. Jaeger, Improved forward model for quantitative pulse-echo speed-of-sound imaging, Ultrasonics (2020) 106168.
[10] S. Krishnan, K. Rigby, M. O'donnell, Improved estimation of phase aberration profiles, IEEE Trans. Ultrason. Ferroelectr. Freq. Control 44 (3) (1997) 701–713.
[11] R. Ali, C.D. Herickhoff, D. Hyun, J.J. Dahl, N. Bottenus, Extending retrospective encoding for robust recovery of the multistatic dataset, IEEE Trans. Ultrason. Ferroelectr. Freq. Control (2019).
[12] T. Harrison, A. Sampaleanu, R.J. Zemp, S-sequence spatially-encoded synthetic aperture ultrasound imaging [correspondence], IEEE Trans. Ultrason. Ferroelectr. Freq. Control 61 (5) (2014) 886–890.
[13] P. Gong, M.C. Kolios, Y. Xu, Delay-encoded transmission and image reconstruction method in synthetic transmit aperture imaging, IEEE Trans. Ultrason. Ferroelectr. Freq. Control 62 (10) (2015) 1745–1756.
[14] M.-H. Bae, M.-K. Jeong, A study of synthetic-aperture imaging with virtual source elements in B-mode ultrasound imaging systems, IEEE Trans. Ultrason. Ferroelectr. Freq. Control 47 (6) (2000) 1510–1519.
[15] J. Shin, L. Huang, J.T. Yen, Spatial prediction filtering for medical ultrasound in aberration and random noise, IEEE Trans. Ultrason. Ferroelectr. Freq. Control 65 (10) (2018) 1845–1856.
[16] K. Dei, B. Byram, The impact of model-based clutter suppression on cluttered, aberrated wavefronts, IEEE Trans. Ultrason. Ferroelectr. Freq. Control 64 (10) (2017) 1450–1464.
[17] L.L. Brickson, D. Hyun, M. Jakovljevic, J.J. Dahl, Reverberation noise suppression in ultrasound channel signals using a 3D fully convolutional neural network, IEEE Trans. Med. Imaging 40 (4) (2021) 1184–1195.
[18] R. Mallart, M. Fink, The van Cittert–Zernike theorem in pulse echo measurements, J. Acoust. Soc. Am. 90 (5) (1991) 2718–2727.
[19] W. Long, N. Bottenus, G.E. Trahey, Incoherent clutter suppression using lag-one coherence, IEEE Trans. Ultrason. Ferroelectr. Freq. Control 67 (8) (2020) 1544–1557.
[20] J.A. Jensen, N.B. Svendsen, Calculation of pressure fields from arbitrarily shaped, apodized, and excited ultrasound transducers, IEEE Trans. Ultrason. Ferroelectr. Freq. Control 39 (2) (1992) 262–267.
[21] J.A. Jensen, Field: A program for simulating ultrasound systems, in: 10th Nordicbaltic Conference on Biomedical Imaging, Vol. 4, Supplement 1, Part 1: 351–353, Citeseer, 1996.
[22] R.J. Fedewa, K.D. Wallace, M.R. Holland, J.R. Jago, G.C. Ng, M.R. Rielly, B.S. Robinson, J.G. Miller, Spatial coherence of backscatter for the nonlinearly produced second harmonic for specific transmit apodizations, IEEE Trans. Ultrason. Ferroelectr. Freq. Control 51 (5) (2004) 576–588.